Received: 22 February 2023 | Revised: 29 May 2023 | Accepted: 31 May 2023

DOI: 10.1111/mec.17048

ORIGINAL ARTICLE

MOLECULAR ECOLOGY WILEY

Sex chromosome heteromorphism and the Fast-X effect in poeciliids

Iulia Darolti[1,2] | Lydia J. M. Fong[1] | Benjamin A. Sandkam[3] | David C. H. Metzger[1] | Judith E. Mank[1]

[1]Department of Zoology and Biodiversity Research Centre, University of British Columbia, Vancouver, British Columbia, Canada

[2]Department of Ecology and Evolution, University of Lausanne, Lausanne, Switzerland

[3]Department of Neurobiology and Behavior, Cornell University, Ithaca, New York, USA

Correspondence
Iulia Darolti, Department of Zoology and Biodiversity Research Centre, University of British Columbia, Vancouver, BC, Canada.
Email: ; iulia.darolti@unil.ch

Funding information
H2020 European Research Council, Grant/Award Number: 680951

Handling Editor: Nick Hamilton Barton

Abstract

Fast-X evolution has been observed in a range of heteromorphic sex chromosomes. However, it remains unclear how early in the process of sex chromosome differentiation the Fast-X effect becomes detectible. Recently, we uncovered an extreme variation in sex chromosome heteromorphism across poeciliid fish species. The common guppy, *Poecilia reticulata*, Endler's guppy, *P. wingei*, swamp guppy, *P. picta* and para guppy, *P. parae*, appear to share the same XY system and exhibit a remarkable range of heteromorphism. Species outside this group lack this sex chromosome system. We combined analyses of sequence divergence and polymorphism data across poeciliids to investigate X chromosome evolution as a function of hemizygosity and reveal the causes for Fast-X effects. Consistent with the extent of Y degeneration in each species, we detect higher rates of divergence on the X relative to autosomes, a signal of Fast-X evolution, in *P. picta* and *P. parae*, species with high levels of X hemizygosity in males. In *P. reticulata*, which exhibits largely homomorphic sex chromosomes and little evidence of hemizygosity, we observe no change in the rate of evolution of X-linked relative to autosomal genes. In *P. wingei*, the species with intermediate sex chromosome differentiation, we see an increase in the rate of nonsynonymous substitutions on the older stratum of divergence only. We also use our comparative approach to test for the time of origin of the sex chromosomes in this clade. Taken together, our study reveals an important role of hemizygosity in Fast-X evolution.

KEYWORDS
hemizygosity, heteromorphy, sex chromosome evolution

1 | INTRODUCTION

Owing to their unusual inheritance pattern and hemizygosity in males, X chromosomes display many distinct evolutionary properties compared to the rest of the genome (Charlesworth et al., 1987; Vicoso & Charlesworth, 2006). The strength of selection and genetic drift, as well as the role of dominance and effective population size, are expected to differ between sex chromosomes and autosomes (Kirkpatrick & Hall, 2004; Mank et al., 2010; Meisel & Connallon, 2013). Comparing differences in the evolution of sex-linked and autosomal loci is important for understanding patterns of mutation and selection acting across the genome.

An elevated rate of coding sequence evolution on the X chromosome relative to the autosomes, referred to as the Fast-X effect (or Fast-Z in the case of ZW systems) has been observed in a diversity of organisms, including humans (Lu & Wu, 2005), primates (Stevenson et al., 2007), mice (Kousathanas et al., 2014), birds (Mank et al., 2007, 2010; Wright et al., 2015), *Drosophila* (Ávila et al., 2014; Charlesworth et al., 2018; Mank et al., 2010), aphids (Jaquiéry et al., 2018), spiders (Bechsgaard et al., 2019) and lepidoptera (Mongue et al., 2022; Pinharanda et al., 2019; Sackton et al., 2014). However, the magnitude of this effect can vary substantially across species due to demographic factors, differences in mating system or regulatory mechanisms acting on the sex chromosomes (Mank et al., 2010). Notably, all the cases of Fast-X above were observed in highly heteromorphic sex chromosomes, where very few genes, if any, remain on the Y chromosome and the X is largely hemizygous in the heterogametic sex. As such, it remains unclear how early in the process of sex chromosome differentiation the Fast-X effect becomes detectible, and how important Y degeneration is in X chromosome evolution (Mrnjavac et al., 2023; Presgraves & Orr, 1998).

There are two potential causes of Fast-X. The single functional copy of the X chromosome in males leads to hemizygous exposure of genes and therefore stronger purifying selection against recessive deleterious mutations and positive selection for recessive beneficial ones expressed in males (Charlesworth et al., 1987). This adaptive cause of Fast-X is mainly expected in species with heteromorphic sex chromosomes and highly degenerated Y chromosomes, as a large proportion of X-linked genes will be hemizygous in males. Alternatively, in every male and female pair, there are only three X chromosomes to four copies of each autosome, although this varies substantially based on mating system and type of heterogamety (Mank et al., 2010; Vicoso & Charlesworth, 2009; Wright et al., 2015; Wright & Mank, 2013). This reduced effective population size of the X relative to the autosomes diminishes the relative power of selection on the X, potentially leading to both greater genetic drift and fixation of weakly deleterious mutations on the X chromosome (Charlesworth et al., 1987). This non-adaptive cause of Fast-X does not necessarily require male hemizygosity, just recombination suppression between the X and Y chromosomes and differences in effective population size between X-linked and autosomal loci, and could apply to X loci where the Y copy is expressed and remains functional. The non-adaptive causes of Fast-X might actually be exacerbated in systems that lack male hemizygosity, as recent theoretical work predicts that in the absence of recombination, recessive deleterious mutations in males can accumulate on young X-linked genes as they become sheltered by the remaining functional Y chromosome gene copies (Mrnjavac et al., 2023).

Recently, we uncovered a case of extreme variation across poeciliids in the rate of sex chromosome degeneration and dosage compensation. The same chromosome pair acts as the XY system in the common guppy, *Poecilia reticulata*, its sister species Endler's guppy, *P. wingei*, the more distantly related swamp guppy, *P. picta*, and the para guppy, *P. parae*, all of which last shared a common ancestor roughly 20 million years ago (Darolti et al., 2019; Sandkam et al., 2021). Notably, *P. latipinna* and *Gambusia holbrooki*, recent outgroup species to this clade, do not show evidence of a sex chromosome system on the same chromosome (Darolti et al., 2019). We therefore hypothesized a recent origin of the system, no more than 20 mya (Figure S1), and sequence data on the Y are consistent with this single origin (Fong et al., 2023). Since this origin, the sex chromosomes of *P. reticulata* and *P. wingei* have remained largely homomorphic, although *P. wingei* shows greater divergence in a limited region (Darolti et al., 2019). For both of these species, although we observe male-specific SNPs in the conserved nonrecombining region (Stratum I), we have observed no evidence of reduced expression of Y gametologs in males (Darolti et al., 2019, 2020). In contrast, the *P. picta* and *P. parae* sex chromosomes are completely nonrecombining (with the exception of a small pseudoautosomal region at the distal end, 20–21 Mb, which comprises ~6% of the chromosome) and the Y chromosome has undergone substantial degeneration, leaving most of the X chromosome in males hemizygous (Darolti et al., 2019; Sandkam et al., 2021). Moreover, *P. picta* and *P. parae* exhibit complete dosage compensation (Darolti et al., 2019; Metzger et al., 2021), which is predicted to accentuate the Fast-X effect (Charlesworth et al., 1987; Mank et al., 2010). The range of sex chromosome differentiation in this clade allows us to investigate patterns of X chromosome coding sequence evolution and to test causes underlying Fast-X effects.

In contrast to hypotheses about a single recent origin, it has recently been proposed that the sex chromosomes of *P. reticulata* represent a recent turnover event, and that the highly diverged *P. picta* and *P. parae* system arose well before the immediate ancestor of *P. parae*, *P. picta*, *P. reticulata* and *P. wingei* (figure 1 from Charlesworth et al., 2021). This model supposes that the homomorphism observed in *P. reticulata* and *P. wingei* represents a turnover event, where the current guppy X and Y chromosomes arose from the ancestral X of *P. picta* (Figure S1). Sex chromosome turnovers are frequent in many animal groups (Bachtrog et al., 2014), so the model is plausible. Disentangling the evolutionary origin of this sex chromosome pair is important for understanding the causes of the observed heterogeneity in sex chromosome differentiation patterns and dosage compensation in this clade.

The signature of Fast-X at internal branches of the phylogeny can be used to date the origin of Y degeneration. If the sex chromosome arose recently in the immediate ancestor of the clade, we might expect Fast-X to be confined to *P. picta* and *P. parae* and internal branches connecting these two species, with Fast-X patterns in *P. reticulata* and *P. wingei* less pronounced or absent, consistent with their far reduced levels of male hemizygosity (Mrnjavac et al., 2023). In contrast, if the sex chromosomes arose much earlier, we might expect Fast-X patterns, evolving over long periods of time in the distant ancestor of the clade, to be evident in internal branches of the phylogeny. Furthermore, molecular signatures of sex chromosome evolution remain evident even after turnover events. For example, the *Drosophila* dot chromosome was ancestrally a highly differentiated sex chromosome that reverted

to an autosome with the emergence of Drosophilidae, and yet it still maintains many of the unique characteristics of a differentiated X chromosome, such as a feminizing effect, non-random gene content and a chromosome-specific gene expression regulatory mechanism (Vicoso & Bachtrog, 2013). Therefore, we might also expect detectible signatures on the X chromosome in species that would have to experience turnovers to new sex chromosomes, *P. reticulata* and *P. wingei*, and those immediate outgroups that would have also had to experience additional turnovers under this hypothesis, with the sex chromosome reverting to autosomes. Our comparative dataset allows us to also test these alternative hypotheses for the origin of the guppy sex chromosomes.

Using a combination of sequence divergence, polymorphism and expression data analyses across poeciliid species, we estimate rates of gene sequence evolution across the genome and assess the presence of Fast-X evolution in each system. Consistent with the extent of Y degeneration, we find significantly higher rates of X coding sequence evolution compared to the autosomes, a signal of Fast-X Evolution, in *P. picta* and *P. parae*, potentially accelerated by the evolution of chromosome-wide dosage compensation in these species. Overall, our results suggest a recent origin of the sex chromosome system in this group.

2 | MATERIALS AND METHODS

2.1 | Sample collection and sequencing

We have previously obtained tissue samples, extracted and sequenced RNA from the tails of three males and three females of *P. reticulata*, *P. wingei*, *P. picta*, *P. parae*, *P. latipinna* and *G. holbrooki* (BioProject IDs PRJNA353986, PRJNA528814, PRJNA741270; Darolti et al., 2019; Metzger et al., 2021; Wright et al., 2017). *P. reticulata* samples were obtained from our outbred laboratory population originating from the Quare River in Trinidad (Kotrschal et al., 2013). *P. wingei* samples were collected from our laboratory population established from a strain maintained by a UK fish fancier. *P. picta* and *P. parae* samples were acquired from Guyana and Suriname, while *P. latipinna* and *G. holbrooki* samples were obtained in Florida. All samples were collected in accordance with national and institutional ethical guidelines.

We extracted RNA from each sample using the Qiagen RNeasy Kit, following the instructions of the manufacturer. Library preparation and sequencing were performed at the University of Oxford Wellcome Centre for Human Genetics and Genome Québec, following standard Illumina protocols and using the Illumina HiSeq 4000 and NextSeq platforms. The data were quality assessed using FastQC v0.11.3 (www.bioinformatics.babraham.ac.uk/projects/fastqc) and trimmed with Trimmomatic v0.36 (Bolger et al., 2014), removing adaptor sequences, reads with an average Phred score of <15 in a sliding window of four bases, reads with leading or trailing bases with a Phred score of <3 and reads shorter than 50 bp following trimming.

2.2 | Identifying orthogroups

For each species, we mapped RNA-seq reads to a previously constructed species-specific female de novo genome assembly (Darolti et al., 2019; Sandkam et al., 2021; Wright et al., 2017) using HISAT2 v2.0.4 (Kim et al., 2015), with the exception of *P. latipinna* for which a male genome assembly was used, and a non-redundant set of transcripts in GTF file format was constructed using StringTie v1.2.4 (Pertea et al., 2015). We filtered the transcripts for non-coding RNA (ncRNA) by extracting transcript sequences with BEDtools getfasta (Quinlan & Hall, 2010) and removing transcripts with a BLAST hit to ncRNA sequences from *Poecilia formosa* (PoeFor_5.1.2), *Oryzias latipes* (MEDAKA1), *Gasterosteus aculeatus* (BROADS1) and *Danio rerio* (GRCz10) from Ensembl 104 (Flicek et al., 2014). Only genes with positional information on chromosomal fragments were kept for further analyses and the longest isoform for each target gene was selected. Lastly, we applied a minimum expression filter of 2 RPKM in at least half of the samples of each sex (minimum of two out of three individuals of either sex), resulting in 13,306 *P. reticulata*, 15,089 *P. wingei*, 13,156 *P. picta*, 24,446 *P. parae*, 14,468 *P. latipinna* and 21,861 *G. holbrooki* genic sequences.

We obtained coding sequences from the outgroup species *P. formosa* (PoeFor_5.1.2), *Xiphophorus maculatus* (Xipmac4.4.2) and *O. latipes* (MEDAKA1) from Ensembl 104 and extracted the longest isoform for each gene. Separately for each of our target species, we determined orthology across target and outgroup sequences using reciprocal BLASTn v2.7.1 (Altschul et al., 1990) with an e-value cut-off of $10e^{-10}$ and a minimum percentage identity of 30%. For genes with multiple blast hits, we chose the top hit based on the highest BLAST score. Our analysis resulted in 7296 *P. reticulata*, 7253 *P. wingei*, 7786 *P. picta*, 9171 *P. parae*, 7251 *P. latipinna* and 6477 *G. holbrooki* orthogroups (four-way 1:1 orthologs).

We tested the robustness of the 1:1 ortholog datasets resulting from the reciprocal BLASTn approach by separately inferring orthologous groups using OrthoFinder (Emms & Kelly, 2019). More than half of the orthogroups recovered using the OrthoFinder approach are shared with the reciprocal BLASTn approach (Figure S4). Restricting the sequence divergence analysis (detailed below) to only orthogroups that are shared between the two approaches revealed similar estimates of rates of divergence to the original estimates based on all orthogroups identified using the reciprocal BLASTn approach (Figure S5). We, therefore, concluded that the reciprocal best-hit datasets were appropriate to use in this case.

2.3 | Estimating sequence divergence across orthogroups

For each contig of each orthogroup, we obtained open reading frames using *O. latipes* (MEDAKA1) protein-coding sequences from Ensembl 104 and BLASTx v2.3.0 with an e-value cut-off of $10e^{-10}$

and a minimum percentage identity of 30%, excluding orthogroups without BLASTx hits or valid protein-coding sequences. We aligned orthologous gene sequences with PRANK v170427 (Löytynoja & Goldman, 2008), using the rooted tree (((Target species, *P. formosa*), *X. maculatus*), *O. latipes*), where the target species was in turn *P. reticulata*, *P. wingei*, *P. picta*, *P. parae*, *P. latipinna* and *G. holbrooki*. Alignments were then filtered to remove gaps.

To avoid false-positive signals of adaptive evolution, poorly aligned or error-rich regions were masked with SWAMP (Harrison et al., 2014). We ran SWAMP twice, first using a threshold of six nonsynonymous substitutions in a window size of 15 codons, and second using a threshold of two and a window size of five. This approach eliminates sequencing errors that cause short stretches of nonsynonymous substitutions as well as alignment errors that cause longer stretches of nonhomologous sequence due to variation in exon splicing or misannotation (Harrison et al., 2014). To select these thresholds, we first applied a range of masking criteria on our datasets. We then ran the branch-site test for positive selection on the target species branches for both the unmasked and masked datasets. We visually inspected the alignments of genes with the highest likelihood ratios and chose the masking criteria that were most efficient at reducing false-positive rates. Finally, we discarded orthologs for which the alignment length was shorter than 300 bp following gap removal and masking, as these likely represent incomplete sequences.

To obtain divergence estimates for each orthogroup and calculate mean d_N/d_S across the target species branch, we used branch model (model = 2, nssites = 0) in the CODEML package in PAML v4.8 (Yang, 2007), using the phylogeny ((Target species#1, *P. formosa*), *X. maculatus*, *O. latipes*), where the target species was successively *P. reticulata*, *P. wingei*, *P. picta*, *P. parae*, *P. latipinna* and *G. holbrooki*. To avoid inaccurate divergence estimates due to mutational saturation and double hits, orthologous genes with $d_S > 2$ were removed from subsequent analyses (Axelsson et al., 2008).

For each of the target species, we divided orthologs into autosomal and sex-linked categories based on their chromosomal location. The sex-linked category excluded genes in the previously identified pseudoautosomal regions (0–5 and >26 Mb of *P. reticulata* chromosome 12; >20 Mb of *P. wingei*, *P. picta*, *P. parae*, *P. latipinna* and *G. holbrooki* chromosomes that are syntenic to the guppy chromosome 12 (Darolti et al., 2019; Sandkam et al., 2021)). In addition, it has recently been discovered that the *P. reticulata* reference genome, which served as reference for scaffold ordering and orientation for our *P. reticulata* de novo genome assembly, has a large inversion on the X chromosome that is specific to the guppy strain on which the reference genome assembly was built and is not present in any of our lab or wild-caught samples (Almeida et al., 2021; Darolti et al., 2020). We thus corrected for this inversion when excluding genes from the PAR and assigning genes to the sex-linked category in *P. reticulata*.

Separately for each genomic category, we extracted the number of nonsynonymous substitutions (D_N), the number of nonsynonymous sites (N), the number of synonymous substitutions (D_S) and the number of synonymous sites (S). Taking into account alignment length, we calculated mean d_N and mean d_S as the ratio of the number of substitutions across all orthologs in that group divided by the number of sites ($d_N = D_N$ /N; $d_S = D_S$/S), thus avoiding bias from short sequences and the issue of infinitely high d_N/d_S estimates due to very low d_S (Mank et al., 2007). We identified significant differences in d_N, d_S and d_N/d_S between genomic categories by subsampling without replacement of the autosomal dataset at the size of the smaller dataset (e.g. X chromosome dataset; Stratum I dataset) using 1000 replicates, and we used bootstrapping with 1000 replicates to determine 95% confidence intervals for each divergence estimate. The strength of the Faster-X effect was calculated for each target species as the ratio of the rate of divergence for the X chromosome over the rate of divergence for the autosomes X(d_N/d_S):A(d_N/d_S).

2.4 | Additional sequence divergence analyses for *P. reticulata*

For comparison to our estimates of rates of divergence based on de novo transcripts, we also estimated rates of sequence evolution in *P. reticulata* using publicly available coding sequences from Ensembl 104 (Guppy_female_1.0_MT). For this analysis, we followed the same steps outlined above in terms of extracting the longest isoform for each gene, identifying orthogroups, aligning target and outgroup sequences, masking and obtaining divergence estimates.

2.5 | Estimating rates of divergence for the ancestral branch to *P. reticulata* and *P. picta*

We performed additional sequence divergence analyses following the same methodology described above but using different phylogenies that allowed us to estimate rates of evolution on the internal branch that is ancestral to *P. reticulata* and *P. picta*. In addition to the *X. maculatus* coding sequences, we obtained sequences for *G. affinis* (ASM309773v1) and *P. latipinna* (P_latipinna-1.0) from Ensembl 105. We used the phylogenies ((*P. reticulata*, *P. picta*)#1, *P. latipinna*, *X. maculatus*) and ((*P. reticulata*, *P. picta*)#1, *G. affinis*, *X. maculatus*) to obtain divergence estimates in PAML. Similarly, we estimated rates of evolution for all the other internal branches of the tree (Figure 2).

2.6 | Polymorphism data

To obtain polymorphism data, for each target species, we first mapped female RNA-seq reads to the genome assembly using the STAR v2.4.2a aligner in two-pass mode (Dobin et al., 2013), and then called SNPs using SAMtools v1.3.1 mpileup (Li et al., 2009) with a minimum base quality of 20 and VarScan v2.3.9 mpileup2snp (Koboldt et al., 2012) with a minimum coverage of two, a minimum average quality of 20, a minimum variant allele frequency of 0.1, *p* value of .05 and strand filter set to 'on'. We next imposed that the polymorphism dataset also passes the filtering criteria used for

calculating rates of sequence divergence. As such, we identified codons for which all sites pass the minimum coverage threshold of 20 in at least half of the individuals (in this case, a minimum of two out of three individuals), there are no alignment gaps following alignment with PRANK, and no ambiguity data (Ns) following masking with SWAMP. To make our dataset compatible for the McDonald–Kreitman test of selection, we only kept genes with both divergence and polymorphism data. We have therefore used the same number of nonsynonymous and synonymous sites in our divergence and polymorphism calculations. We identified whether SNPs were synonymous or nonsynonymous by matching them to the reading frame using custom scripts (available at https://github.com/manklab/Darolti_etal_2022_FastX_evolution). For each genomic category, we calculated mean p_N and mean p_S as the ratio of the number of polymorphisms across all orthologs in that group divided by the number of sites ($p_N = P_N/N$; $p_S = P_S/S$).

2.7 | Testing for selection using divergence and polymorphism data

For each species, we estimated the number of genes evolving under neutral and adaptive evolution using the McDonald–Kreitman test (McDonald & Kreitman, 1991). Neutral theory predicts that the ratio of nonsynonymous to synonymous changes within species (p_N/p_S) should be equal to that between species (d_N/d_S) (McDonald & Kreitman, 1991). As such, the McDonald–Kreitman test identifies signatures of positive selection, where there is an excess of nonsynonymous substitutions relative to polymorphisms ($d_N/d_S > p_N/p_S$), and of relaxed purifying selection, where there is a deficit of nonsynonymous substitutions compared to polymorphisms ($d_N/d_S < p_N/p_S$). To test for deviations from neutrality, for each contig, we used a 2×2 contingency table and a Fisher's Exact Test in R v3.6.2 (R Core Team, 2015). The power of the McDonald–Kreitman test is limited with low table counts, therefore we restricted this analysis to genes for which the sum of each row and column in the contingency table was equal to or greater than six (Andolfatto, 2008; Begun et al., 2007).

As the McDonald–Kreitman test is a very conservative test, we also used the divergence and polymorphism data to calculate the direction of selection statistic (DoS; Stoletzki & Eyre-Walker, 2011). For each gene, we calculated the difference between the proportion of nonsynonymous substitutions and polymorphisms ($DoS = D_N(D_N + D_S) - P_N(P_N + P_S)$), where positive DoS values are indicative of positive selection. We used Fisher's Exact test in R to test for significant differences in the proportion of genes under positive selection between the autosomes and the X chromosome in each species.

Lastly, we used the polymorphism data alone to test for an excess or deficit of nonsynonymous polymorphisms on the X chromosome compared to the autosomes, which would suggest a relaxed constraint or purifying selection respectively. For this, we concatenated P_N and P_S estimates within each species and used Fisher's Exact test in R to test for significant differences in P_N/P_S between the autosomes and the X chromosome.

3 | RESULTS

3.1 | Fast-X evolution in the heteromorphic sex chromosomes of *P. picta* and *P. parae*

We first assessed the strength of Fast-X in our study species with heteromorphic sex chromosomes. The extensive X chromosome hemizygosity of *P. picta* and *P. parae* males is expected to accentuate the strength of Fast-X evolution in these species (Vicoso & Charlesworth, 2006), as is the mechanism of complete X chromosome dosage compensation (Mank et al., 2010). Indeed, our analysis in *P. picta* and *P. parae* revealed a higher rate of nonsynonymous substitutions for X-linked loci, excluding genes in the pseudoautosomal region (PAR) (see Section 2), compared to the autosomes (1000 replicates permutation test, $p < .001$; Table S1). Both species also exhibit a significantly elevated rate of divergence (d_N/d_S) on the X chromosome relative to the rest of the genome (Figure 1c,d), consistent with a signal of Fast-X evolution (Figure 2; Figure S2) measured as the ratio of the rate of nonsynonymous over synonymous substitutions for the X chromosome relative to that for the autosomes. The rates of divergence for loci in the PAR were not different from those of autosomal loci (Table S1). Our results thus indicate that the Fast-X signal is present in both *P. picta* and *P. parae*.

3.2 | Absence of Fast-X effect in species with homomorphic sex chromosomes

We next asked whether patterns of coding sequence evolution are different between the species with heteromorphic sex chromosomes, *P. picta* and *P. parae* and the species with homomorphic sex chromosomes, *P. reticulata* and *P. wingei*. Previous work has indicated that *P. reticulata* and *P. wingei* share the same XY sex chromosome system (Darolti et al., 2019; Morris et al., 2018; Nanda et al., 2014). Analyses of coverage differences between males and females indicate that Y degeneration is restricted to the distal end of the sex chromosomes, in a region ancestral to *P. reticulata* and *P. wingei* (designated as Stratum I) (Darolti et al., 2019, 2020; Fraser et al., 2020; Qiu et al., 2022; Wright et al., 2017), and suggest that Y degeneration is slightly more exaggerated in *P. wingei* compared to *P. reticulata*. This nonrecombining region coincides with the previously mapped location of the sex determining region in *P. reticulata* (Traut & Winking, 2001; Tripathi et al., 2009; Winge, 1922, 1927; Winge & Ditlevsen, 1947) and is also found across six natural guppy populations from Trinidad (Almeida et al., 2021).

We, therefore, assessed the signal of Fast-X evolution for genes in Stratum I (20–26 Mb on *P. reticulata* chromosome 12; 17–20 Mb on *P. wingei* chromosome syntenic to the guppy sex chromosome). In *P.*

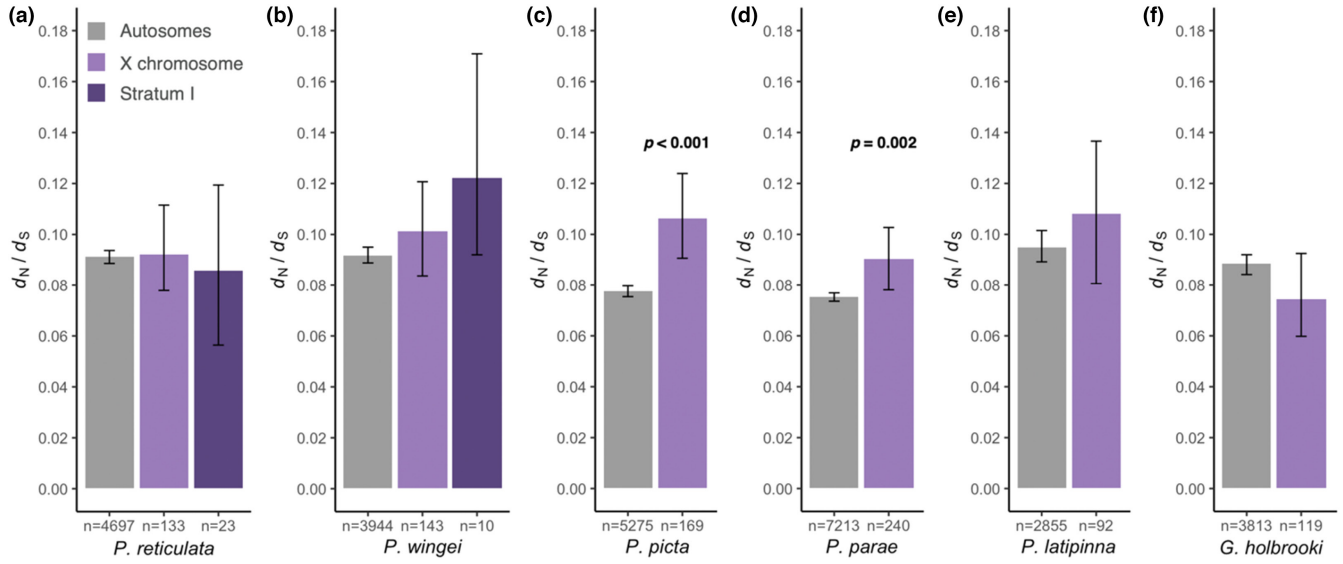

FIGURE 1 Estimates of the rate of divergence (d_N/d_S) for autosomal and X-linked genes in (a) *Poecilia reticulata*, (b) *P. wingei*, (c) *P. picta*, (d) *P. parae*, (e) *P. latipinna* and (f) *Gambusia holbrooki*. For all species, the X chromosome category excludes genes on the PAR. Additionally, in *P. reticulata* and *P. wingei*, the X chromosome category excludes genes in Stratum I. In *P. latipinna* and *G. holbrooki*, the X chromosome represents the chromosome syntenic to guppy chromosome 12. 95% confidence intervals are based on bootstrapping with 1000 replicates. Differences between autosomal and X-linked loci are based on 1000 replicate permutation tests. Only significant differences are shown (*p* value <.01).

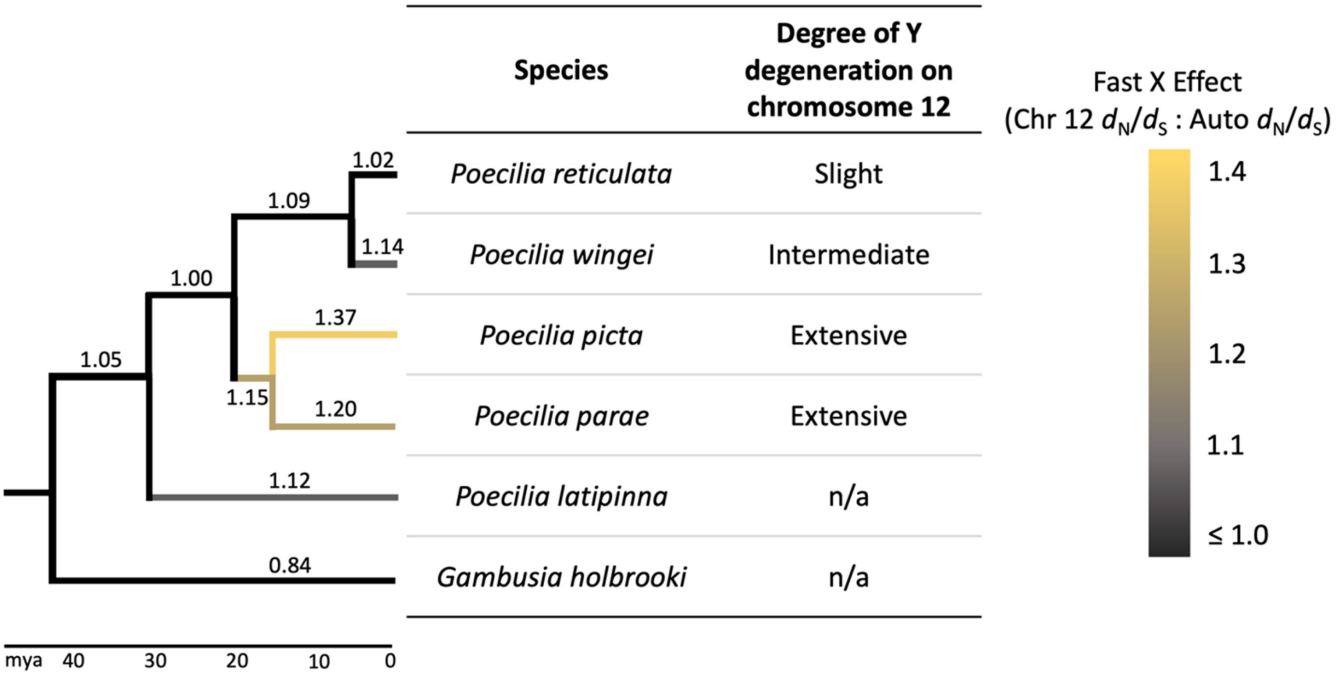

FIGURE 2 Fast-X effect, calculated as the ratio of d_N/d_S for the X chromosome (excluding the PAR) to that of the autosomes, across the poeciliids. In *Poecilia latipinna* and *Gambusia holbrooki*, chromosome 12 has not been implicated as the sex chromosome. Numbers on each branch represent the estimated Fast-X effect. Phylogeny based on Meredith et al. (2010) and Rabosky et al. (2018).

reticulata, the rate of divergence for X-linked genes in Stratum I was not significantly different than that for autosomal genes (Figure 1a; Table S1). To exclude the possibility that we were lacking power in our analysis due to the small number of genes identified in Stratum I, we reanalysed *P. reticulata* using Ensembl coding sequences instead of our de novo generated transcripts. We were able to recover more than twice as many X-linked loci, however, the estimates of divergence remain the same as those based on de novo transcripts (Figure S3).

In contrast to *P. reticulata*, we find a significantly higher rate of nonsynonymous substitutions for genes in Stratum I compared to autosomal loci in *P. wingei* (Table S1); however, the overall rate

of divergence is similar between the autosomes and Stratum I (Figure 1b). Recent work has suggested that the *P. wingei* X and Y chromosomes are somewhat more differentiated from each other compared to those of *P. reticulata* (Darolti et al., 2019), and there is also evidence for this from previous cytogenetic work (Nanda et al., 1992, 2014). This greater divergence might explain the difference in d_N estimates for X-linked genes in Stratum I that we observe between these two species, though the effect is negligible. However, it should be noted that following filtering (see Section 2), only a handful of *P. wingei* genes remained in Stratum I, and as such our statistical power to detect a significant Fast-X signal in this species is reduced.

3.3 | Ancestral Fast-X

If the ancestor of the guppy and *P. picta* had an almost completely degenerated sex chromosome system and had evolved dosage compensation (as suggested in the model by Charlesworth et al., 2021), then a signal of Fast-X evolution would have also accumulated prior to the species split. We might expect this pattern to manifest at internal branches of the phylogeny in the ancestor of *P. parae*, *P.picta*, *P. reticulata* and *P.wingei*, and even before the split of this group from the *P. latipinna* or the *Gambusia* clade. We ran separate phylogenetic analyses with different outgroup species, however neither recovered any difference in the overall rate of divergence or the rates of either nonsynonymous or synonymous substitutions between the autosomal and sex-linked gene categories (Table 1; Figure 2). This indicates the absence of a Fast-X signal in the branch that is ancestral to *P. reticulata*, *P. wingei*, *P. picta* and *P. parae*, suggesting large-scale Y degeneration and hemizygosity evolved in the immediate ancestor of *P. picta* and *P. parae*.

The molecular and evolutionary signatures that accumulate on sex chromosomes remain observable even when they revert to being autosomes (Vicoso & Bachtrog, 2013), and we might therefore expect the pattern of Fast-X that we observed in *P. picta* and *P. parae* to still be observed throughout the *P. reticulata* and *P. wingei* sex chromosomes outside of Stratum I if they were paired with highly degenerated Y chromosomes before turnover events. Thus, we next estimated rates of sequence divergence for the remainder of the X chromosome, excluding genes in Stratum I and genes on the PAR (see Section 2), as the high recombination events in the PAR can alter rates of evolution and polymorphism (Otto et al., 2011). Although the Fast-X effect was >1 in *P. wingei* (Figure 2; Figure S2), mean d_N/d_S for genes on the X chromosome was not significantly different from genes on the autosomes in either *P. reticulata* or *P. wingei* (Figure 1a,b; Table S1).

It has been proposed that the large-scale Y gene loss observed in *P. picta* would have taken considerable amounts of time, much more than the time since *P. picta* split from *P. reticulata* (Charlesworth et al., 2021), estimated at ~20 mya (Meredith et al., 2010; Rabosky et al., 2018). If that is the case, the Turnover Model also requires additional sex chromosome turnover events in *P. latipinna*, an outgroup species to the *P. reticulata*–*P. wingei* which has split from *P. parae* only ~26 mya (Meredith et al., 2010; Rabosky et al., 2018), if not also in the more distantly related *G. holbrooki* (Figure S2). We therefore estimated sequence divergence in the outgroups, *P. latipinna* and *G. holbrooki*, both species in which the guppy chromosome 12 has not been implicated as the sex chromosome, and found no evidence of elevated rates of evolution on the chromosome syntenic to the guppy X relative to the rest of the genome in either species (Table S1).

3.4 | Polymorphism and the underlying causes of Fast-X

A higher d_N/d_S on the X chromosome relative to the rest of the genome could be the result of both increased genetic drift (Charlesworth et al., 1987; Mank et al., 2010) and increased efficacy of selection (Vicoso & Charlesworth, 2009). Therefore, we used sequence and polymorphism data together to test for the causes of elevated Fast-X evolution in *P. picta* and *P. parae*. The McDonald–Kreitman test contrasts the number of nonsynonymous and synonymous substitutions with polymorphisms, where an excess of nonsynonymous substitutions relative to polymorphisms is indicative of positive selection (McDonald & Kreitman, 1991). Using this test, we detected no X-linked genes with signatures of positive selection in any of the poeciliid species.

The McDonald–Kreitman test is very conservative, as it is restricted to genes with sufficient numbers of substitutions and polymorphisms (Andolfatto, 2008; Begun et al., 2007), and as such, our analysis was limited to a few X-linked contigs. To increase our

TABLE 1 Divergence estimates for autosomal and X-linked genes on the ancestral branch to *P. reticulata* and *P. picta*.

Phylogeny	Category	No. genes	Sum D_N (mean per gene)	Sum D_S (mean per gene)	d_N (95% CI)	d_S (95% CI)	d_N/d_S (95% CI)
(((*P. reticulata*, *P. picta*), *P. latipinna*), *X. maculatus*)	Autosomes	2213	3065 (1.4)	7453 (3.4)	0.0013 (0.0013–0.0014)	0.0094 (0.0092–0.0097)	0.1422 (0.1338–0.1507)
	X chromosome	82	111 (1.4)	272 (3.3)	0.0014 (0.0010–0.0018)	0.0096 (0.0085–0.0110)	0.1416 (0.1016–0.1937)
(((*P. reticulata*, *P. picta*), *G. affinis*), *X. maculatus*)	Autosomes	3654	17,410 (4.8)	53,719 (14.7)	0.0049 (0.0048–0.0051)	0.0451 (0.0444–0.0457)	0.1093 (0.1055–0.1130)
	X chromosome	127	658 (5.2)	2047 (16.1)	0.0052 (0.0044–0.0061)	0.0477 (0.0441–0.0510)	0.1096 (0.0924–0.1299)

Note: The X chromosome category excludes genes on the PAR. 95% confidence intervals are based on bootstrapping with 1000 replicates.

statistical power to detect signatures of positive selection, we also used the direction of selection (DoS) test which is less sensitive to low counts (Stoletzki & Eyre-Walker, 2011). For each contig, DoS calculates the difference between the proportion of nonsynonymous substitutions and the proportion of nonsynonymous polymorphisms, where a positive DoS indicates adaptive evolution (Stoletzki & Eyre-Walker, 2011). Using this approach, we recovered more genes with signatures of positive selection, however the X chromosome was not enriched in these genes compared to the rest of the genome in any of the species (Table S3; Figure S6).

We next used polymorphism data alone to test for the efficacy of selection acting on the X chromosome. A higher rate of nonsynonymous to synonymous polymorphisms on the X relative to the autosomes is indicative of reduced efficacy of selection to remove mildly deleterious mutations, while a lower rate suggests selection acts more strongly on the X chromosome due to hemizygous exposure to remove deleterious mutations in males. Our results show a lower rate of nonsynonymous polymorphisms on the X chromosome in *P. picta* and *P. parae* only (Table 2, 1000 replicates permutation tests $p = .04$ for *P. picta* and $p = .03$ for *P. parae*; Table S2), suggesting selection is better able to remove mildly deleterious variation on highly differentiated sex chromosomes (Charlesworth et al., 1987; Vicoso & Charlesworth, 2009).

4 | DISCUSSION

4.1 | The role of hemizygosity in Fast-X

There are two potential causes of Fast-X evolution. Male heterogamety leads to hemizygous exposure of genes resulting in stronger purifying selection against recessive deleterious mutations and positive selection for recessive beneficial ones expressed in males (Charlesworth et al., 1987). Alternatively, the reduced effective population size of the X relative to the autosomes diminishes the relative power of selection on the X, potentially leading to non-adaptive causes of Fast-X (Charlesworth et al., 1987). This does not necessarily require male hemizygosity (Presgraves & Orr, 1998), just recombination suppression between the X and Y chromosomes. In the absence of recombination, young homomorphic sex chromosomes may additionally experience a Fast-X effect as recessive deleterious mutations accumulate on X-linked loci due to sheltering by the functional gene copies on the Y chromosome (Mrnjavac et al., 2023).

We observe a clear pattern of Fast-X in *P. picta* and *P. parae*, as shown through the significantly higher rate of nonsynonymous substitutions for X-linked loci (Table S1) and the significantly elevated rate of divergence on the X chromosome relative to the rest of the genome (Figures 1c,d and 2), consistent with the degree of heteromorphism and extensive Y chromosome degeneration in this species. In contrast, we did not observe the accumulation of mutations on X-linked loci or significant patterns of Fast-X evolution for the homomorphic sex chromosomes in *P. reticulata* and *P. wingei*. It is possible that incomplete X-Y recombination suppression in these species is preventing deleterious mutations from accumulating on the X chromosome (Darolti et al., 2020), and there is little evidence of loss of Y gene coding sequence (Darolti et al., 2019, 2020), with very few, if any, genes being hemizygously expressed in males, even in the older Stratum I. Interestingly, in *P. wingei*, the Y is somewhat more diverged than the Y in *P. reticulata* (Darolti et al., 2019; Nanda et al., 1992, 2014), and we observe a slight, though non-significant Fast-X effect in Stratum I in the former. All these point to the key role of sex chromosome hemizygosity in driving Fast-X evolution in poeciliids.

Some previous work has failed to detect X-Y divergence based on male: female coverage differences in Stratum I of *Poecilia*

TABLE 2 Polymorphism estimates for autosomal and X-linked genes across poeciliid species.

Species	Category	No. genes	p_N (95% CI)	p_S (95% CI)	p_N/p_S (95% CI)
P. reticulata	Autosomes	2211	.0012 (0.0011–0.0012)	.0110 (0.0105–0.0113)	.1054 (0.0980–0.1134)
	X chromosome	74	.0012 (0.0008–0.0016)	.0131 (0.0109–0.0159)	.0883 (0.0591–0.1225)
P. wingei	Autosomes	934	.0009 (0.0008–0.0010)	.0077 (0.0071–0.0082)	.1155 (0.1036–0.1275)
	X chromosome	34	.0008 (0.0004–0.0012)	.0103 (0.0080–0.0130)	.0791 (0.0411–0.1257)
P. picta	Autosomes	1485	.0006 (0.0006–0.0007)	.0051 (0.0048–0.0053)	.1191 (0.1082–0.1311)
	X chromosome	40	.0003 (0.0002–0.0006)	.0043 (0.0030–0.0061)	.0790 (0.0438–0.1293)
P. parae	Autosomes	4167	.0010 (0.0009–0.0011)	.0078 (0.0076–0.0080)	.1307 (0.1249–0.1365)
	X chromosome	123	.0007 (0.0006–0.0009)	**.0059 (0.0049–0.0068)**	.1301 (0.0983–0.1776)
P. latipinna	Autosomes	1041	.0010 (0.0009–0.0011)	.0095 (0.0089–0.0100)	.1081 (0.1082–0.1311)
	Chromosome syntenic to guppy X	35	.0016 (0.0010–0.0024)	.0111 (0.0081–0.0147)	.1452 (0.0832–0.2469)
G. holbrooki	Autosomes	1464	.0014 (0.0013–0.0015)	.0155 (0.0146–0.0163)	.0872 (0.0800–0.0947)
	Chromosome syntenic to guppy X	42	.0013 (0.0008–0.0018)	.0191 (0.0153–0.0234)	.0659 (0.0410–0.0990)

Note: Only genes with both divergence and polymorphism data are included in this analysis. For all species, the X chromosome category excludes genes on the PAR. 95% confidence intervals are based on bootstrapping with 1000 replicates. Differences between autosomal and sex-linked categories are based on 1000 replicate permutation tests and significant differences are indicated by bold values ($p < .01$).

reticulata (Bergero et al., 2019; Charlesworth et al., 2020; Kirkpatrick et al., 2022). However, studies that have used similar genomic methods across a range of datasets all recovered patterns consistent with this region (Almeida et al., 2021; Darolti et al., 2019; Fraser et al., 2020; Sigeman et al., 2022; Wright et al., 2017), as have studies using male-specific sequence (Almeida et al., 2021; Darolti et al., 2020; Morris et al., 2018). A recent methodological analysis revealed that the detection of Stratum I in *P. reticulata* is largely dependent upon the reference genome used (Darolti et al., 2022), with studies using reference genomes from distant populations or even different species less able to detect subtle patterns of divergence that characterize the Y chromosome in this species. Our detection of a slight, but non-significant pattern of Fast-X in Stratum I of the *P. wingei* X chromosome gives further weight to the presence of this Stratum.

In addition to the effects of hemizygosity, effective population size and sheltering, theory predicts that complete dosage compensation, whereby balance in expression between the sex chromosomes and the autosomes is restored, may facilitate a more pronounced Fast-X effect (Charlesworth et al., 1987; Mank et al., 2010). Under this theory, in systems with incomplete dosage compensation, where only a subset of the genes are compensated for but overall expression for X-linked genes is reduced compared to the autosomes in males, X-linked beneficial mutations may have lower expression and weaker phenotypic effects in males, potentially limiting the Fast-X effect (Charlesworth et al., 1987; Mank et al., 2010). *P. picta* and *P. parae* have evolved chromosome-wide dosage compensation, seemingly through a mechanism involving the hyperexpression of the single X in males (Darolti et al., 2019; Metzger et al., 2021), and this could have contributed to the observed signature of Fast-X evolution.

The role of hemizygosity in *P. picta* and *P. parae* Fast-X suggests a greater efficacy of selection acting in males to remove recessive deleterious variation. However, although we were unable to differentiate adaptive and non-adaptive causes of Fast-X in our polymorphism data, polymorphism estimates are sensitive to demographic fluctuations (Pool & Nielsen, 2007; Tajima, 1989) and, thus, it is difficult to determine to what extent the Fast-X pattern in *P. picta* is adaptive using polymorphism data alone. Future work identifying true X-hemizygous loci in males and analysing their patterns of sequence evolution may prove more revealing.

4.2 | Differentiating between models of sex chromosome origin

Different models have been proposed for the origin of the sex chromosome system in this group. Based on parsimony, the presence of the sex chromosomes of Guppy Chromosome 12 in *P. reticulata*, *P. wingei*, *P. picta* and *P. parae*, and the absence of sex chromosomes on all outgroup poeciliids suggest that this sex chromosomes system arose once roughly 20 mya and subsequently experienced different rates of Y decay in different sub-clades (Darolti et al., 2019; Fong et al., 2023), possibly exacerbated by the evolution of complete dosage compensation in the immediate ancestor of *P. picta* and *P. parae* (Lenormand et al., 2020; Metzger et al., 2021; Sandkam et al., 2021). Others have speculated about a much earlier origin, well before the immediate ancestor of *P. parae*, *P. picta*, *P. reticulata* and *P. wingei*, and large-scale Y degeneration and complete dosage compensation occurred before the most recent common ancestor of the four species (Charlesworth et al., 2021).

Overall, our results are consistent with a recent origin of the sex chromosome system. Our branch-specific analysis revealed that Fast-X is largely confined to the immediate ancestor of *P. picta* and *P. parae*, consistent with rapid origin of X chromosome dosage compensation in the immediate ancestor of this clade, which reduces selection to maintain Y chromosome expression for dosage-sensitive genes (Metzger et al., 2021). We also failed to recover signatures of Fast-X in *P. reticulata* and *P. wingei* that would be consistent with an ancient origin. Our data cannot be used to test more complicated recent origin hypotheses of two separate origins on the same chromosome pair, once in the ancestor of *P. picta* and *P. parae*, and another in the ancestor of *P. reticulata* and *P. wingei* (Kirkpatrick et al., 2022), although Y sequence data from across the clade are consistent with a single recent origin (Fong et al., 2023).

5 | CONCLUDING REMARKS

Taken together, our comparative analyses of divergence and polymorphism data across poeciliids reveal that the degree of Fast-X evolution follows the extent of X hemizygosity in males, emphasizing the important role of male hemizygosity in this evolutionary process. Our results across the broader clade are consistent with a recent origin of the sex chromosome system, as opposed to an ancient origin with turnovers. This indicates that patterns of Fast-X evolution can accumulate rapidly in the evolution of sex chromosomes.

AUTHOR CONTRIBUTIONS

Judith E. Mank and Iulia Darolti designed the research. Iulia Darolti, Lydia J. M. Fong, Benjamin A. Sandkam, David C. H. Metzger and Judith E. Mank performed the data analysis and contributed to the writing of the manuscript.

ACKNOWLEDGEMENTS

This work was supported by the European Research Council (grant agreement 680951), a Canada 150 Research Chair and an NSERC Discovery Grant to J.E.M. We thank the members of the Mank lab and two anonymous reviewers for helpful and constructive suggestions on the manuscript.

CONFLICT OF INTEREST STATEMENT

The authors declare no conflict of interest.

DATA AVAILABILITY STATEMENT

Scripts used for data processing and analysis are available at https://github.com/manklab/Darolti_etal_MolEcol_2023_FastX_evolution and are archived on Zenodo (https://doi.org/10.5281/zenodo.8020460).

ORCID

Iulia Darolti https://orcid.org/0000-0002-5865-4969
Benjamin A. Sandkam https://orcid.org/0000-0002-5043-9295
David C. H. Metzger https://orcid.org/0000-0001-7552-1204
Judith E. Mank https://orcid.org/0000-0002-2450-513X

REFERENCES

Almeida, P., Sandkam, B. A., Morris, J., Darolti, I., Breden, F., & Mank, J. E. (2021). Divergence and remarkable diversity of the Y chromosome in guppies. *Molecular Biology and Evolution*, *38*, 619–633.

Altschul, S. F., Gish, W., Miller, W., Myers, E., & Lipman, D. J. (1990). Basic local alignment search tool. *Journal of Molecular Biology*, *215*, 403–410.

Andolfatto, P. (2008). Controlling type-I error of the McDonald–Kreitman test in Genomewide scans for selection on noncoding DNA. *Genetics*, *180*, 1767–1771.

Ávila, V., De Procé, S. M., Campos, J. L., Borthwick, H., Charlesworth, B., & Betancourt, A. J. (2014). Faster-X effects in two drosophila lineages. *Genome Biology and Evolution*, *6*, 2968–2982.

Axelsson, E., Hultin-Rosenberg, L., Brandström, M., Zwahlén, M., Clayton, D. F., & Ellegren, H. (2008). Natural selection in avian protein-coding genes expressed in brain. *Molecular Ecology*, *17*, 3008–3017.

Bachtrog, D., Mank, J. E., Peichel, C. L., Kirkpatrick, M., Otto, S. P., Ashman, T. L., Hahn, M. W., Kitano, J., Mayrose, I., Ming, R., Perrin, N., Ross, L., Valenzuela, N., Vamosi, J. C., & The Tree of Sex Consortium. (2014). Sex determination: Why so many ways of doing it? *PLoS Biology*, *12*, e1001899.

Bechsgaard, J., Schou, M. F., Vanthournout, B., Hendrickx, F., Knudsen, B., Settepani, V., Schierup, M. H., & Bilde, T. (2019). Evidence for faster X chromosome evolution in spiders. *Molecular Biology and Evolution*, *36*, 1281–1293.

Begun, D. J., Holloway, A. K., Stevens, K., Hillier, L. W., Poh, Y. P., Hahn, M. W., Nista, P. M., Jones, C. D., Kern, A. D., Dewey, C. N., Pachter, L., Myers, E., & Langley, C. H. (2007). Population genomics: Whole-genome analysis of polymorphism and divergence in *Drosophila simulans*. *PLoS Biology*, *5*, 2534–2559.

Bergero, R., Gardner, J., Bader, B., Yong, L., & Charlesworth, D. (2019). Exaggerated heterochiasmy in a fish with sex-linked male coloration polymorphisms. *Proceedings of the National Academy of Sciences of the United States of America*, *116*, 6924–6931.

Bolger, A. M., Lohse, M., & Usadel, B. (2014). Trimmomatic: A flexible trimmer for Illumina sequence data. *Bioinformatics*, *30*, 2114–2120.

Charlesworth, B., Campos, J. L., & Jackson, B. C. (2018). Theory and evidence from *Drosophila*. *Molecular Ecology*, *27*, 3753–3771.

Charlesworth, B., Coyne, J. A., & Barton, N. H. (1987). The relative rates of evolution of sex chromosomes and autosomes. *The American Naturalist*, *130*, 113–146.

Charlesworth, D., Bergero, R., Graham, C., Gardner, J., & Keegan, H. (2021). How did the guppy Y chromosome evolve? *PLoS Genetics*, *17*, e1009704.

Charlesworth, D., Bergero, R., Graham, C., Gardner, J., & Yong, L. (2020). Locating the sex determining region of linkage group 12 of guppy (*Poecilia reticulata*). *G3: Genes – Genomes – Genetics*, *10*, 3639–3649.

Darolti, I., Almeida, P., Wright, A. E., & Mank, J. E. (2022). A comparison of methodological approaches to the study of young sex chromosomes: A case study in *Poecilia*. *Journal of Evolutionary Biology*, *35*, 1646–1658. https://doi.org/10.1111/jeb.14013

Darolti, I., Wright, A. E., & Mank, J. E. (2020). Guppy Y chromosome integrity maintained by incomplete recombination suppression. *Genome Biology and Evolution*, *12*, 965–977.

Darolti, I., Wright, A. E., Sandkam, B. A., Morris, J., Bloch, N. I., Farré, M., Fuller, R. C., Bourne, G. R., Larkin, D. M., Breden, F., & Mank, J. E. (2019). Extreme heterogeneity in sex chromosome differentiation and dosage compensation in livebearers. *Proceedings of the National Academy of Sciences of the United States of America*, *116*, 19031–19036.

Dobin, A., Davis, C. A., Schlesinger, F., Drenkow, J., Zaleski, C., Jha, S., Batut, P., Chaisson, M., & Gingeras, T. R. (2013). STAR: ultrafast universal RNA-seq aligner. *Bioinformatics*, *29*, 15–21.

Emms, D. M., & Kelly, S. (2019). OrthoFinder: Phylogenetic orthology inference for comparative genomics. *Genome Biology and Evolution*, *20*, 1–14.

Flicek, P., Amode, M. R., Barrell, D., Beal, K., Billis, K., Brent, S., Carvalho-Silva, D., Clapham, P., Coates, G., Fitzgerald, S., Gil, L., Girón, C. G., Gordon, L., Hourlier, T., Hunt, S., Johnson, N., Juettemann, T., Kähäri, A. K., Keenan, S., … Searle, S. M. J. (2014). Ensembl 2014. *Nucleic Acids Research*, *42*, 749–755.

Fong, L. J. M., Darolti, I., Metger, D. C. H., Morris, J., Lin, Y., Sandkam, B. A., & Mank, J. E. (2023). Evolutionary history of the *Poecilia picta* sex chromosomes. *Genome Biology and Evolution*, *15*, evad030.

Fraser, B. A., Whiting, J. R., Paris, J. R., Weadick, C. J., Parsons, P. J., Charlesworth, D., Bergero, R., Bemm, F., Hoffmann, M., Kottler, V. A., Liu, C., Dreyer, C., & Weigel, D. (2020). Improved reference genome uncovers novel sex-linked regions in the guppy (*Poecilia reticulata*). *Genome Biology and Evolution*, *12*, 1789–1805.

Harrison, P. W., Jordan, G. E., & Montgomery, S. H. (2014). SWAMP: Sliding window alignment masker for PAML. *Evolutionary Bioinformatics*, *10*, 197–204.

Jaquiéry, J., Peccoud, J., Ouisse, T., Legeai, F., Prunier-Leterme, N., Gouin, A., Nouhaud, P., Brisson, J. A., Bickel, R., Purandare, S., Poulain, J., Battail, C., Lemaitre, C., Mieuzet, L., le Trionnaire, G., Simon, J. C., & Rispe, C. (2018). Disentangling the causes for Faster-X evolution in aphids. *Genome Biology and Evolution*, *10*, 507–520.

Kim, D., Langmead, B., & Salzberg, S. L. (2015). HISAT: A fast spliced aligner with low memory requirements. *Nature Methods*, *12*, 357–360.

Kirkpatrick, M., & Hall, D. W. (2004). Male-biased mutation, sex linkage, and the rate of adaptive evolution. *Evolution*, *58*, 437–440.

Kirkpatrick, M., Sardell, J. M., Pinto, B. J., Dixon, G., Peichel, C. L., & Schartl, M. (2022). Evolution of the canonical sex chromosomes of the guppy and relatives. *G3: Genes – Genomes – Genetics*, *12*, jkab435.

Koboldt, D. C., Zhang, Q., Larson, D. E., Shen, D., McLellan, M. D., Lin, L., Miller, C. A., Mardis, E. R., Ding, L., & Wilson, R. K. (2012). VarScan 2: Somatic mutation and copy number alteration discovery in cancer by exome sequencing. *Genome Research*, *22*, 568–576.

Kotrschal, A., Rogell, B., Bundsen, A., Svensson, B., Zajitschek, S., Immler, S., Maklakov, A. A., & Kolm, N. (2013). Experimental evidence for costs and benefits of evolving a larger brain. *Current Biology*, *23*, 168–171.

Kousathanas, A., Halligan, D. L., & Keightley, P. D. (2014). Faster-X adaptive protein evolution in house mice. *Genetics*, *196*, 1131–1143.

Lenormand, T., Fyon, F., Sun, E., & Roze, D. (2020). Sex chromosome degenration by regulatory evolution. *Current Biology*, *30*, 3001–3006. e3005.

Li, H., Handsaker, B., Wysoker, A., Fennell, T., Ruan, J., Homer, N., Marth, G., Abecasis, G., & Durbin, R. (2009). The sequence alignment/map format and SAMtools. *Bioinformatics*, *25*, 2078–2079.

Löytynoja, A., & Goldman, N. (2008). Phylogeny-aware gap replacement prevents errors in sequence alignment and evolutionary analysis. *Science*, *320*, 1632–1635.

Lu, J., & Wu, C.-I. (2005). Weak selection revealed by the whole-genome comparison of the X chromosome and autosomes of human and chimpanzee. *Proceedings of the National Academy of Sciences of the United States of America*, *102*, 4063–4067.
Mank, J. E., Axelsson, E., & Ellegren, H. (2007). Fast-X on the Z: Rapid evolution of sex-linked genes in birds. *Genome Research*, *17*, 618–624.
Mank, J. E., Vicoso, B., Berlin, S., & Charlesworth, B. (2010). Effective population size and the faster-X effect: Empirical results and their interpretation. *Evolution*, *64*, 663–674.
McDonald, J. H., & Kreitman, M. (1991). Adaptive protein evolution at the ADH locus in *Drosophila*. *Nature*, *351*, 652–654.
Meisel, R. P., & Connallon, T. (2013). The faster-X effect: Integrating theory and data. *Trends in Genetics*, *29*, 537–544.
Meredith, R. W., Pires, M. N., Reznick, D. N., & Springer, M. S. (2010). Molecular phylogenetic relationships and the evolution of the placenta in *Poecilia* (Micropoecilia) (Poeciliidae: Cyprinodontiformes). *Molecular Phylogenetics and Evolution*, *55*, 631–639.
Metzger, D. C. H., Sandkam, B. A., Darolti, I., & Mank, J. E. (2021). Rapid evolution of complete dosage compensation in *Poecilia*. *Genome Biology and Evolution*, *13*, evab155.
Mongue, A. J., Hansen, M. E., & Walters, J. R. (2022). Support for faster and more adaptive Z chromosome evolution in two divergent lepidopteran lineages. *Evolution*, *76*, 332–345.
Morris, J., Darolti, I., Bloch, N. I., Wright, A. E., & Mank, J. E. (2018). Shared and species-specific patterns of nascent Y chromosome evolution in two guppy species. *Genes*, *9*, 238.
Mrnjavac, A., Khudiakova, K. A., Barton, N. H., & Vicoso, B. (2023). Slower-X: Reduced efficiency of selection in the early stages of X chromosome evolution. *Evolution Letters*, *31*, 4–12.
Nanda, I., Schartl, M., Feichtinger, W., Epplen, J. T., & Schmid, M. (1992). Early stages of sex chromosome differentiation in fish as analysed by simple repetitive DNA sequences. *Chromosoma*, *101*, 301–310.
Nanda, I., Schories, S., Tripathi, N., Dreyer, C., Haaf, T., Schmid, M., & Schartl, M. (2014). Sex chromosome polymorphism in guppies. *Chromosoma*, *123*, 373–383.
Otto, S. P., Pannell, J. R., Peichel, C. L., Ashman, T.-L., Charlesworth, D., Chippindale, A. K., Delph, L. F., Guerrero, R. F., Scarpino, S. V., & McAllister, B. F. (2011). About PAR: The distinct evolutionary dynamics of the pseudoautosomal region. *Trends in Genetics*, *27*, 358–367.
Pertea, M., Pertea, G. M., Antonescu, C. M., Chang, T. C., Mendell, J. T., & Salzberg, S. L. (2015). StringTie enables improved reconstruction of a transcriptome from RNA-seq reads. *Nature Biotechnology*, *33*, 290–295.
Pinharanda, A., Rousselle, M., Martin, S. H., Hanly, J. J., Davey, J. W., Kumar, S., Galtier, N., & Jiggins, C. D. (2019). Sexually dimorphic gene expression and transcriptome evolution provide mixed evidence for a fast-Z effect in *Heliconius*. *Journal of Evolutionary Biology*, *32*, 194–204.
Pool, J. E., & Nielsen, R. (2007). Population size changes reshape genomic patterns of diversity. *Journal of Evolutionary Biology*, *61*, 30001–33006.
Presgraves, D. C., & Orr, H. A. (1998). Haldane's rule in taxa lacking a hemizygous X chromosome. *Science*, *282*, 962–954.
Qiu, S., Yong, L., Wilson, A., Croft, D. P., Graham, C., & Charlesworth, D. (2022). Partial sex linkage and linkage disequilibrium on the guppy sex chromosome. *BioRxiv*. https://doi.org/10.1101/2022.01.14.476360
Quinlan, A. R., & Hall, I. M. (2010). Genome analysis BEDTools: A flexible suite of utilities for comparing genomic features. *Bioinformatics*, *26*, 841–842.
R Core Team. (2015). *R: A language and environment for statistical computing*. R Foundation for Statistical Computing. https://www.r-project.org
Rabosky, D. L., Chang, J., Cowman, P. F., Sallan, L., Friedman, M., Kascher, K., Garilao, C., Near, T. J., Coll, M., & Alfaro, M. E. (2018). An inverse latitudinal gradient in speciation rate for marine fishes. *Nature*, *559*, 392–395.
Sackton, T. B., Corbett-Detig, R. B., Nagaraju, J., Vaishna, L., Arunkumar, K. P., & Hartl, D. L. (2014). Positive selection drives faster-Z evolution in silkmoths. *Evolution*, *68*, 2331–2342.
Sandkam, B. A., Almeida, P., Darolti, I., Furman, B. L. S., van der Bijl, W., Morris, J., Bourne, G. R., Breden, F., & Mank, J. E. (2021). Extreme Y chromosome polymorphism corresponds to five male reproductive morphs of a freshwater fish. *Nature Ecology & Evolution*, *5*, 939–948.
Sigeman, H., Sinclair, B., & Hansson, B. (2022). FindZX: An automated pipeline for detecting and visualising sex chromosomes using whole-genome sequencing data. *BMC Genomics*, *23*, 328.
Stevenson, B. J., Iseli, C., Panji, S., Zahn-Zabal, M., Hide, W., Old, L. J., Simpson, A. J., & Jongeneel, C. V. (2007). Rapid evolution of cancer/testis genes on the X chromosome. *BMC Genomics*, *8*, 1–11.
Stoletzki, N., & Eyre-Walker, A. (2011). Estimation of the neutrality index. *Molecular Biology and Evolution*, *28*, 63–70.
Tajima, F. (1989). The effect of change in population size on DNA polymorphism. *Genetics*, *123*, 597–601.
Traut, W., & Winking, H. (2001). Meiotic chromosomes and stages of sex chromosome evolution in fish: Zebrafish, platyfish and guppy. *Chromosome Research*, *9*, 659–672.
Tripathi, N., Hoffmann, M., Willing, E. M., Lanz, C., Weigel, D., & Dreyer, C. (2009). Genetic linkage map of the guppy, *Poecilia reticulata*, and quantitative trait loci analysis of male size and colour variation. *Proceedings of the Biological Sciences*, *276*, 2195–2208.
Vicoso, B., & Bachtrog, D. (2013). Reversal of an ancient sex chromosome to an autosome in drosophila. *Nature*, *499*, 332–335.
Vicoso, B., & Charlesworth, B. (2006). Evolution on the X chromosome: Unusual patterns and processes. *Nature Reviews. Genetics*, *7*, 645–653.
Vicoso, B., & Charlesworth, B. (2009). The deficit of male-biased genes on the *D. melanogaster* X chromosome is expression-dependent: A consequence of dosage compensation? *Journal of Molecular Evolution*, *68*, 576–583.
Winge, Ö. (1922). One-sided masculine and sex-linked inheritance in *Lebistes reticulatus*. *Journal of Genetics*, *12*, 145–162.
Winge, Ö. (1927). The location of eighteen genes in *Lebistes reticulatus*. *Journal of Genetics*, *18*, 1–43.
Winge, Ö., & Ditlevsen, E. (1947). Colour inheritance and sex determination in *Lebistes*. *Heredity*, *1*, 65–83.
Wright, A. E., Darolti, I., Bloch, N. I., Oostra, V., Sandkam, B., Buechel, S. D., Kolm, N., Breden, F., Vicoso, B., & Mank, J. E. (2017). Convergent recombination suppression suggests role of sexual selection in guppy sex chromosome formation. *Nature Communications*, *8*, 14251.
Wright, A. E., Harrison, P. W., Zimmer, F., Montgomery, S. H., Pointer, M. A., & Mank, J. E. (2015). Variation in promiscuity and sexual selection drives avian rate of faster-Z evolution. *Molecular Ecology*, *24*, 1218–1235.
Wright, A. E., & Mank, J. E. (2013). The scope and strength of sex-specific selection in genome evolution. *Journal of Evolutionary Biology*, *26*, 1841–1853.
Yang, Z. (2007). PAML 4: Phylogenetic analysis by maximum likelihood. *Molecular Biology and Evolution*, *24*, 1586–1591.

SUPPORTING INFORMATION

Additional supporting information can be found online in the Supporting Information section at the end of this article.

How to cite this article: Darolti, I., Fong, L. J. M., Sandkam, B. A., Metzger, D. C. H., & Mank, J. E. (2023). Sex chromosome heteromorphism and the Fast-X effect in poeciliids. *Molecular Ecology*, *32*, 4599–4609. https://doi.org/10.1111/mec.17048